Combustion and Flame 254 (2023) 112852

Contents lists available at ScienceDirect

Combustion and Flame

journal homepage: www.elsevier.com/locate/combustflame

Cool diffusion flames in a stably stratified stagnation flow

Kendyl A. Waddell[a], Han Ju Lee[a], Vedha Nayagam[b], Richard L. Axelbaum[c], Peter B. Sunderland[a,*]

[a] Department of Fire Protection Engineering, University of Maryland, College Park, MD 20742, USA
[b] Department of Mechanical and Aerospace Engineering, Case Western Reserve University, Cleveland, OH 44106, USA
[c] Department of Energy, Environmental & Chemical Engineering, Washington University in St. Louis, St. Louis, MO 63130, USA

ARTICLE INFO

Article history:
Received 21 July 2022
Revised 13 May 2023
Accepted 14 May 2023

Keywords:
Low-temperature combustion
Negative-temperature coefficient
n-Heptane
Pool fires

ABSTRACT

Cool diffusion flames have been a growing research topic since their discovery in 2012. Until now their study has been hindered by the high cost of the experimental systems used to observe them. A method is presented here for observing cool diffusion flames inexpensively using a pool of liquid *n*-heptane and parallel plates heated so as to produce a stably stratified stagnation flow. The flames were imaged with a color camera and an intensified camera. Measurements included gas phase temperatures, fuel evaporation rates, and formaldehyde yields. These are the first observations of cool flames burning near the surfaces of fuel pools. The measured peak temperatures were between 705 and 760 K and were 70 K above the temperature of the surrounding air. Autoignition first occurred at 550 K.

1. Introduction

Despite recent advances in renewable energy, the world is still highly dependent on fossil fuel combustion for energy production. The need for cleaner and more efficient engines is imperative. Advances in internal combustion engine processes could help meet this need. Recently, low-emission engine technologies such as homogeneous charge compression ignition (HCCI), premixed charge compression ignition (PCCI), and reactivity controlled compression ignition (RCCI) have been pursued. In these engines, autoignition via cool flames is an integral part of the combustion process [1–4], but this process is not sufficiently understood. The thermal efficiency of current internal-combustion engines, typically 38%, could be increased to 60% with future ultra-lean and low-temperature engines that exploit cool flames [5].

Premixed cool flames were first observed in the early 19th century [6]. Their understanding has since evolved alongside advances in experimental and numerical techniques. Cool flames have peak temperatures of 500–1000 K and increase the local gas temperature on the order of 100 K [5]. They consume just a fraction of the reactants, and produce formaldehyde [7,8].

The existence of cool diffusion flames (CDFs) had been predicted by Cuoci et al. [9], but they were not observed until 2012, in droplet experiments aboard the International Space Station (ISS) [10]. The two-stage burning that was observed on the ISS was numerically confirmed to be associated with CDFs [11].

This discovery of CDFs has led to a surge of interest in cool flame research. CDFs have been observed in microgravity with droplets of various fuels [12–15] and with a spherical porous burner [16]. They have also been observed in normal gravity counterflow flames [17–21]. Unfortunately, the spherical CDFs require costly long-duration microgravity, and past work in counterflow CDFs has involved cool flame enhancers (ozone addition, plasmas, or enriched oxygen), which perturb the fundamental chemistry.

Many of these studies used *n*-heptane as a fuel. Stable CDFs are favored when the fuel is a large alkane or an ether. Due to the low reaction rates they also require long residence times, which can be achieved using stagnation flow [17,22]. Temperatures must be elevated to slightly below the negative-temperature coefficient region, increasing the radical pool in the flame and helping the radical-deprived CDF autoignite [23]. Most CDFs stabilize on the rich side [12–16,18,19,21].

Modeled temperatures of CDFs are far more prevalent than measured. Won et al. [17] measured and predicted *n*-heptane CDF peak temperatures of 640 and 828 K in counterflow CDFs. The temperatures predicted for droplets have been in between: Seshadri et al. [24] predicted a cool flame crossover temperature of 770 K and Farouk et al. [11] predicted a cool flame temperature of 700 K.

A common theme of past observations of CDFs is that the burners or facilities used are available to only a limited number of researchers worldwide. This inhibits the potential for widespread research on CDFs. This study seeks to develop an inexpensive experimental setup for observing CDFs.

* Corresponding author.
E-mail address: pbs@umd.edu (P.B. Sunderland).

https://doi.org/10.1016/j.combustflame.2023.112852
0010-2180/

2. Experimental

The burner apparatus is illustrated in Fig. 1. The fuel is *n*-heptane, which has a molar mass of 100.2 g/mol, a boiling point of 372 K, and a flash point of 269 K [25]. This is contained in a PYREX borosilicate glass beaker with a capacity of 30 mL and an inner diameter of 32 mm. The beaker is placed on the lower heater, a flat cast iron heater with a diameter of 188 mm (Cusimax model CMHP-B101, 1.5 kW at 110 VAC). A second Cusimax heater (the upper heater) is inverted and mounted above the annular disk. The heater excitations (11–110 VAC) were controlled with external variable transformers. The lower heater is primarily used to heat the liquid *n*-heptane, while the upper heater is primarily used to heat the gas above the pool.

An annular aluminum disk, with a thickness of 3.3 mm, an inner diameter of 32 mm, and an outer diameter of 146 mm, is secured to the top of the beaker. The annular disk helps stabilize the CDFs, in regions with good optical access, by reducing unsteady flows near the reaction zone. It also provides uniform temperatures and long residence times near the reaction zone and allows more independent temperature control with the two heaters. The separation distance, S, between the annular disk and the upper heater was varied from 1 to 15 mm.

The burner apparatus is installed in a rectangular hood with a footprint of 100 $\times$ 100 cm, a height of 60 cm, the front face open, and a vent flow rate of 2400 LPM. All the tests were in air at 1.01 bar.

The CDFs burned above the opening in the annular disk. Fuel vapor arrived at the reaction zone mainly by convection, as shown by streamlines in Fig. 1, while the oxidizer arrived mainly by diffusion. CDFs have extensive fuel and oxidizer leakage across the reaction zone. Although the gas was stably stratified above the annular disk, recirculation zones there are likely at such low bulk flow velocities.

Images were recorded with a Nikon D5300 digital color camera with a Nikkor 50 mm lens. Because the CDFs were dim, and barely visible to the naked eye, the f/# was 1.4, the ISO was 12,800, and the exposure time was 1 s. A Xybion ISG-750 intensified video camera was also used for real-time visual observations of the CDFs at 30 frames/s.

Temperatures were measured using three 250 μm diameter type K (nickel/chromium/alumel) uncoated bare-wire thermocouples. Two were in fixed locations in contact with the upper heater and disk at a radius of 20 mm. The third was in and near the CDFs, and for some tests it was translated radially or vertically. Because the thermocouple readings were low, and relatively close to the temperatures of the heater and disk, no radiation corrections were made. The uncertainty in measured temperatures is estimated at $\pm$5 K.

The *n*-heptane evaporation rates were measured gravimetrically, with an estimated uncertainty of $\pm$10%. Formaldehyde concentrations at the entrance to the exhaust vent were measured with a Temtop LKC-1000E formaldehyde sensor, with an estimated uncertainty of $\pm$1 ppm.

Each measurement was performed several times to confirm repeatability. The uncertainties stated herein consider both the measurement variance and estimates of bias.

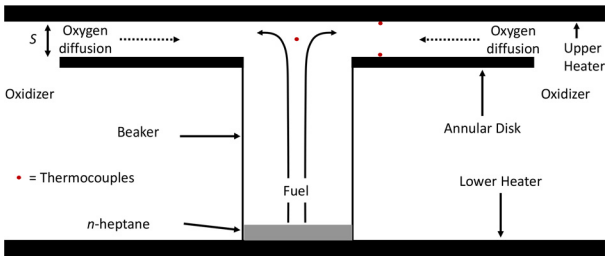

Fig. 1. Schematic of the burner apparatus showing approximate streamlines.

3. Results

3.1. Flame appearance and formaldehyde yields

With the heaters, beaker, and disk in thermal equilibrium, and the desired S established, the beaker and disk were removed and quickly returned after 1 mL of *n*-heptane was added to the beaker. For S between 5 and 10 mm, a CDF autoignited after 2–5 s and burned continuously until the fuel was depleted. The CDFs were nearly steady, but there was occasional flame motion. Continuously burning CDFs were not observed for S outside this range. Instead, the CDFs would fluctuate, extinguish, and reignite. For CDFs the pool temperature was maintained near 343 K to avoid fuel flow rates that were too low or too high for stable CDFs.

Figure 2 shows representative images of three CDFs for various S. These flames were blue (because of excited formaldehyde) and so dim they could only be seen in a darkened laboratory. The CDF shapes varied with S. For S = 5 mm (see Fig. 2) the CDF was nearly flat with slight upward concavity. Its main reaction zone extended from the beaker centerline to nearly the disk walls. For S = 7.5 mm, the flame base was at the height of the annular disk and at a radius of 6.5 mm. The main reaction zone curved upward and outward. For S = 10 mm, the brightest part of the CDF was much wider. At this S the CDFs were less steady. Stable CDFs were not observed for S below 5 mm or above 10 mm.

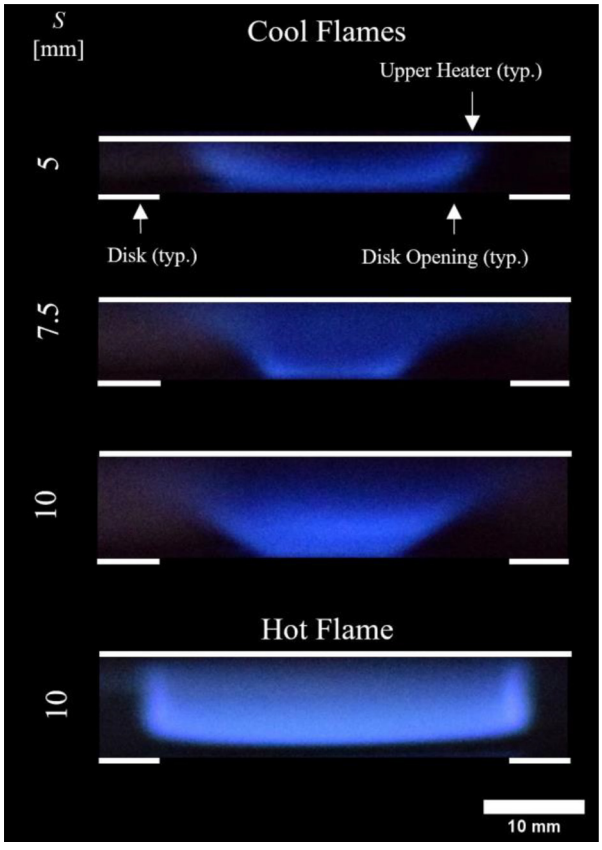

Fig. 2. Color images of representative *n*-heptane flames. The exposure times were 1 s and 10 ms for the cool and hot flames, respectively.

Autoignition to hot flames was not observed for any of these flames unless the upper heater was hotter than 800 K or an external butane flame was introduced. For $S < 10$ mm, the hot flame flashed briefly before being replaced by a CDF. For S between 10 and 12.5 mm, a blue hot flame burned for a few seconds but then extinguished and was replaced by a CDF. For $S > 12.5$ mm, a yellow, sooting hot flame appeared and burned until the fuel was depleted. It is noteworthy that only CDFs (i.e., not hot flames) burned continuously for $S < 12.5$ mm. For these conditions the hot flames were quenched by the upper heater surfaces, whereas these surfaces have temperatures closer to the peak CDF temperatures.

A representative hot flame image is shown in Fig. 2. The hot flames were visible under normal ambient lighting, and were about 140 times as luminous as the CDFs.

The measured *n*-heptane evaporation rates were 1.1 and 2.2 mg/s for CDFs and hot flames, respectively, and these were independent of S for the CDFs. Based on this, the gas velocities in the beaker (assuming *n*-heptane vapor at 600 K) were 0.65 and 1.3 mm/s for the CDFs and the hot flames, respectively. The increased evaporation rates for the hot flames resulted from heat feedback from the flame to the pool.

When CDFs were present, the measured formaldehyde concentration in the vent line was 2 ppm. Considering the vent flow rate and the *n*-heptane evaporation rate, and assuming all products are well mixed at the vent entrance, this corresponds to a formaldehyde yield of 0.1 g/g-fuel. The hot flames did not produce a detectable level (0.01 ppm or higher) of formaldehyde.

3.2. Temperatures

For some tests the thermocouple was translated vertically along the burner axis. Results for representative tests are shown in Fig. 3a. The temperature between the upper heater and the disk opening varied by 60 and 30 K for the no-fuel and CDF cases, respectively. The same power was supplied to the upper heater in both cases. Extrapolating these curves to the upper heater indicates its temperature on the axis was 640 and 710 K for the no-fuel and CDF cases, respectively.

For some tests the thermocouple was translated radially at the mid-plane between the disk and the upper heater. The results for the two cases in Fig. 3a are shown in Fig. 3b. This CDF had a peak temperature of 700 K (as determined from the mean of the left and right peaks in Fig. 3b). This behavior is unlike that for the hot flames, whose temperatures exceeded the thermocouple limit of 1533 K.

Figure 4 shows the measured peak CDF temperatures plotted with respect to S. For these tests the same power was supplied to the upper heater as in Fig. 3. The temperatures in Fig. 4 increase linearly with increasing S. This behavior could result from variations in CDF equivalence ratios and/or heat losses via conduction to the metal surfaces or radiation. Increasing S is expected to decrease the equivalence ratio near the CDF by increasing the area available for oxygen to diffuse upstream. Zhao et al. [23] predicted that premixed cool flame temperatures increase with increasing equivalence ratio, but the measurements of Hajilou et al. [26] and Brown et al. [27] in premixed flames indicate the opposite.

To observe the ignition and extinction of these CDFs, the temperature of the upper heater was ramped up and then down for some tests. This was performed both with and without fuel in the beaker. The upper heater and disk had the same temperatures whether or not fuel (and a CDF) were present at fixed heater power. These CDFs were at times unsteady or extinguished, and thus were observed with the intensified video camera.

The resulting temperatures for a representative test are shown in Fig. 5. When no fuel was present, the gas temperature ramped up to 610 K and then decreased. When fuel was present, exothermic cool flame reactions commenced when the gas temperature first reached 560 K, and the gas temperature quickly increased by about 100 K upon ignition. The initial CDF was weak, and sharp oscillations in CDF temperature are seen in Fig. 5. As the heater temperature increased, the CDF strengthened and reached a peak temperature of 710 K. Then, as the heater cooled, the CDF cooled, then fluctuated in position with occasional extinction and re-ignition events, as evidenced by sharp 60 K swings in gas temperature. The gas temperature fluctuations after ignition and before extinction could not be eliminated with slower temperature ramping. When the gas temperature dropped below 560 K, the CDF extinguished and did not reignite. This test, and similar tests at other S, indicate that these CDFs ignited and extinguished at 550 ± 20 K, and that their peak temperatures increased with increasing temperature of the upper heater.

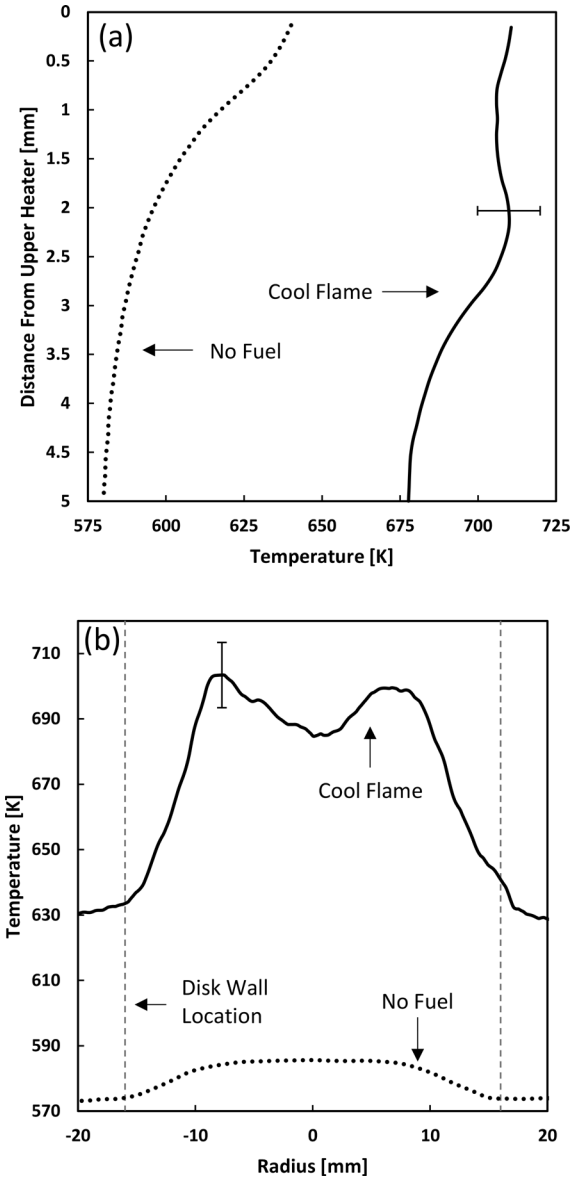

Fig. 3. (a) Gas temperatures on the burner axis versus distance from the upper heater for $S = 5$ mm. (b) Gas temperatures versus radius with $S = 5$ mm and with the thermocouple 2.5 mm below the upper heater.

The measured CDF temperatures of Figs. 3–5 are among the first for *n*-heptane CDFs. The measured peak temperatures are in a similar range to those of past measurements and predictions [11,17,24]. These measurements provide support for past state-

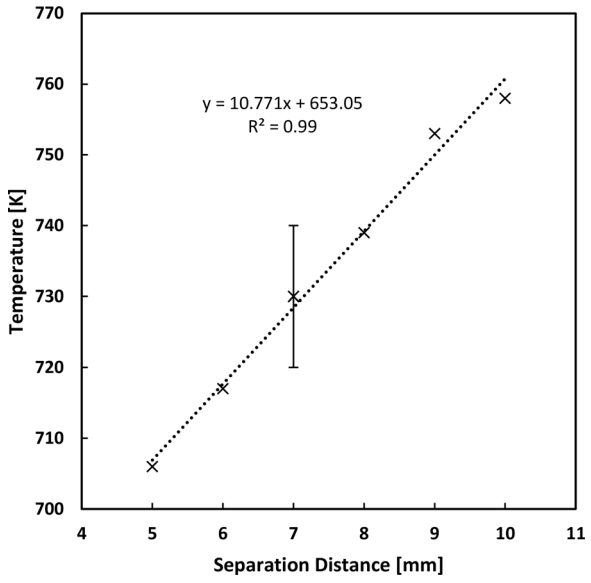

Fig. 4. Peak temperatures of the CDFs as a function of *S*. The thermocouple was at a distance of 0.5 *S* below the upper heater and at the radius of maximum temperature.

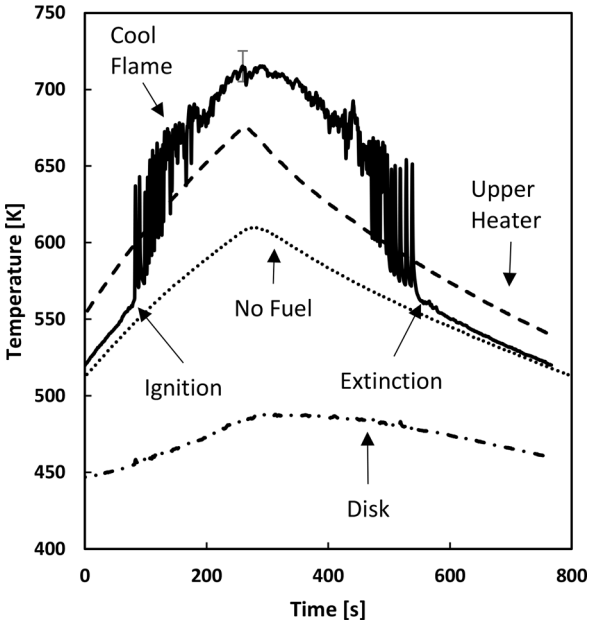

Fig. 5. Gas, heater, and disk temperatures versus time for $S = 5$ mm. The gas temperatures were measured 2.5 mm from the upper heater and at a radius of 8 mm. The heater and disk temperatures were measured at a radius of 20 mm.

ments that cool flames increase the local gas temperature on the order of 100 K [5,17]. In particular, in Fig. 3b the peak CDF temperature is 70 K above the temperature of the surrounding air, while in Fig. 5 the initial ignition of a CDF increases the peak temperature by 80 K.

4. Conclusions

Cool diffusion flames were observed burning *n*-heptane in a stably-stratified stagnation flow. The flames burned between parallel plates with various separation distances. The measurements included flame imaging, gas temperatures, evaporation rates, and formaldehyde emissions. The main conclusions are as follows.

This configuration using a stably-stratified stagnation flow is an inexpensive alternative to most past experiments of CDFs. For separation distances of 5–10 mm, the CDFs burned until the fuel was depleted.

The peak temperatures of the CDFs were between 705 and 760 K, increased with increasing separation distance, and were 70 K above the temperature of the surrounding air. The CDFs autoignited at a temperature of 550 K.

The *n*-heptane evaporation rate was 1.1 mg/s and the formaldehyde yield was 0.1 g/g-fuel.

Hot flames were also observed using the same apparatus. These had much higher temperatures, 140 times the luminosity, twice the *n*-heptane evaporation rate, and no formaldehyde emissions. For a separation distance below 12.5 mm, any hot flames extinguished and were replaced by CDFs.

This new approach to generating CDFs, being something that can be easily accomplished in any lab without cool flame enhancers such as ozone, plasmas, or enriched oxygen, should be valuable for future studies of CDFs.

Declaration of Competing Interest

The authors declare that they have no known competing financial interests or personal relationships that could have appeared to influence the work reported in this paper.

Acknowledgments

This research was funded by NSF grant CBET1740490. The authors are grateful for the assistance of Forman Williams and James Baldwin.

References

[1] M. Yao, Z. Zheng, H. Liu, Progress and recent trends in homogeneous charge compression ignition (HCCI) engines, Prog. Energy Combust. Sci. 35 (2009) 398–437.
[2] C.S. Yoo, T. Lu, J.H. Chen, C.K. Law, Direct numerical simulations of ignition of a lean n-heptane/air mixture with temperature inhomogeneities at constant volume: parametric study, Combust. Flame 158 (2011) 1727–1741.
[3] R.D. Reitz, Directions in internal combustion engine research, Combust. Flame 160 (2013) 1–8.
[4] T. Jin, Y. Wu, X. Wang, K.H. Luo, T. Lu, K. Luo, J. Fan, Ignition dynamics of DME/methane-air reactive mixing layer under reactivity controlled compression ignition conditions: effects of cool flames, Appl. Energy 249 (2019) 343–354.
[5] Y. Ju, Understanding cool flames and warm flames, Proc. Combust. Inst. 38 (2021) 83–119.
[6] H. Davy, VIII Some new experiments and observations on the combustion of gaseous mixtures, with an account of a method of preserving a continued light in mixtures of inflammable gases and air without flame, Philos. Trans. R. Soc. Lond. 107 (1817) 77–85.
[7] P.G. Lignola, E. Reverchon, Cool flames, Prog. Energy Combust. Sci. 13 (1987) 75–96.
[8] G. Paczko, N. Peters, K. Seshadri, F.A. Williams, The role of cool-flame chemistry in quasi-steady combustion and extinction of *n*- heptane droplets, Combust. Theory Model. 18 (2014) 515–531.
[9] A. Cuoci, M. Mehl, G. Buzzi-Ferraris, T. Faravelli, D. Manca, E. Ranzi, Autoignition and burning rates of fuel droplets under microgravity, Combust. Flame 143 (2005) 211–226.
[10] V. Nayagam, D.L. Dietrich, P.V. Ferkul, M.C. Hicks, F.A. Williams, Can cool flames support quasi-steady alkane droplet burning? Combust. Flame 159 (2012) 3583–3588.
[11] T.I. Farouk, F.L. Dryer, Isolated n-heptane droplet combustion in microgravity: “cool flames” – two-stage combustion, Combust. Flame 161 (2014) 565–581.
[12] V. Nayagam, D.L. Dietrich, M.C. Hicks, F.A. Williams, Cool-flame extinction during n-alkane droplet combustion in microgravity, Combust. Flame 162 (2015) 2140–2147.
[13] D.L. Dietrich, R. Calabria, P. Massoli, V. Nayagam, F.A. Williams, Experimental observations of the low-temperature burning of decane/hexanol droplets in microgravity, Combust. Sci. Technol. 189 (2017) 520–554.
[14] T.I. Farouk, D. Dietrich, F.L. Dryer, Three stage cool flame droplet burning behavior of *n*-alkane droplets at elevated pressure conditions: hot, warm and cool flame, Proc. Combust. Inst. 37 (2019) 3353–3361.
[15] V. Nayagam, F.A. Williams, D.L. Dietrich, Asymptotic analysis of cool-flame propagation in mixtures of an *n*-alkane, oxygen, and nitrogen, Combust. Theory Model. 26 (2021) 1–13.

[16] M. Kim, K.A. Waddell, P.B. Sunderland, V. Nayagam, D.P. Stocker, D.L. Dietrich, Y. Ju, F.A. Williams, P.H. Irace, R.L. Axelbaum, Spherical gas-fueled cool diffusion flames, Proc. Combust. Inst. 39 (2023).
[17] S.H. Won, B. Jiang, P. Diévart, C.H. Sohn, Y. Ju, Self-sustaining n -heptane cool diffusion flames activated by ozone, Proc. Combust. Inst. 35 (2015) 881–888.
[18] C.B. Reuter, M. Lee, S.H. Won, Y. Ju, Study of the low-temperature reactivity of large n-alkanes through cool diffusion flame extinction, Combust. Flame 179 (2017) 23–32.
[19] C.H. Sohn, H.S. Han, C.B. Reuter, Y. Ju, S.H. Won, Thermo-kinetic dynamics of near-limit cool diffusion flames, Proc. Combust. Inst. 36 (2017) 1329–1337.
[20] A. Alfazazi, A. Al-Omier, A. Secco, H. Selim, Y. Ju, S.M. Sarathy, Cool diffusion flames of butane isomers activated by ozone in the counterflow, Combust. Flame 191 (2018) 175–186.
[21] O.R. Yehia, C.B. Reuter, Y. Ju, On the chemical characteristics and dynamics of n-alkane low-temperature multistage diffusion flames, Proc. Combust. Inst. 37 (2019) 1717–1724.
[22] M. Lee, Y. Fan, Y. Ju, Y. Suzuki, Ignition characteristics of premixed cool flames on a heated wall, Combust. Flame 231 (2021) 111476.
[23] P. Zhao, C.K. Law, The role of global and detailed kinetics in the first-stage ignition delay in NTC-affected phenomena, Combust. Flame 160 (2013) 2352–2358.
[24] K. Seshadri, N. Peters, F.A. Williams, V. Nayagam, G. Paczko, Asymptotic analysis of quasi-steady *n* -heptane droplet combustion supported by cool-flame chemistry, Combust. Theory Model. 20 (2016) 1118–1130.
[25] PubChem, Compound summary for CID 15600, decane, (2022).
[26] M. Hajilou, M.Q. Brown, M.C. Brown, E. Belmont, Investigation of the structure and propagation speeds of n-heptane cool flames, Combust. Flame 208 (2019) 99–109.
[27] M.C. Brown, E.L. Belmont, Experimental characterization of ozone-enhanced *n*-decane cool flames and numerical investigation of equivalence ratio dependence, Combust. Flame 230 (2021) 111429.